Transformation of carbendazim induced by the H_2O_2/UV system in the presence of hydrogenocarbonate ions : involvement of the carbonate radical

Patrick Mazellier,* Émilie Leroy, Joseph De Laat and Bernard Legube

Laboratoire de Chimie de l'Eau et de l'Environnement (CNRS UMR 6008), Université de Poitiers ESIP, 40 Avenue du Recteur Pineau, 86022, Poitiers, France. E-mail: Patrick.Mazellier@univ-poitiers.fr; Fax: +33 5 49 45 37 68; Tel: +33 5 49 45 39 15

Received (in Montpellier, France) 3rd May 2002, Accepted 3rd September 2002
First published as an Advance Article on the web 29th October 2002

The transformation of the fungicide carbendazim by hydroxyl radicals generated by the photolysis ($\lambda_{exc.} = 254$ nm) of hydrogen peroxide in aqueous solution has been studied in the absence and in the presence of hydrogenocarbonate ions. In the presence of high concentrations of hydrogen peroxide, the second-order rate constant of the reaction of $HO^\bullet$ radicals with carbendazim has been determined to be equal to $(2.2 \pm 0.3) \times 10^9$ L.mol^{-1}.s^{-1}. The identification of the main degradation by-products shows the existence of two different reaction sites for carbendazim induced degradation: the benzene ring and the methyl group. Good simulations of carbendazim disappearance have been obtained by kinetic modelling over a wide range of initial H_2O_2 concentrations. In the presence of hydrogenocarbonate ions, a quenching effect is observed and the simulations lead to an underestimation of the carbendazim disappearance. This is because of the involvement of the carbonate radicals, which react with carbendazim with a second-order rate constant evaluated to be equal to $(6 \pm 2) \times 10^6$ L.mol^{-1}.s^{-1} by kinetic modelling. When the starting concentration of HCO_3^- is high enough, the elimination of carbendazim by $CO_3^{\bullet}$ becomes the major route of carbendazim transformation.

Hydroxyl radicals may be formed in the aquatic environment by different photolytic pathways involving iron(III), nitrate ions or natural organic matter. In water treatment, the oxidation of organic pollutants can be achieved with various processes involving ozone, hydrogen peroxide and ultraviolet radiation, and their coupling (Advanced Oxidation Processes). In most of the cases, the efficiency of these processes is due to the generation of $HO^\bullet$ radicals. The hydroxyl radical is a very powerful oxidant (standard reduction potential equal to 2.72 and 1.89 V *vs.* SHE at pH = 0 and 14, respectively[1]) and is able to react with organic pollutants with high second-order rate constants (10^7–10^{10} M^{-1}.s^{-1} depending on the chemical structure of the pollutant). The combination of hydrogen peroxide with UV provides a simple way to generate hydroxyl radicals without additional secondary chemical reactions[2] and has been the subject of numerous investigations. Kinetic modeling of oxidation reactions using this system appears relatively easy to achieve in various experimental conditions.[3–5]

In the presence of hydrogenocarbonate/carbonate ions, hydroxyl radical leads to the formation of carbonate radical. This latter radical is a strong one-electron oxidant (1.59 V *vs.* SHE at pH = 12[6]). It has been considered for a long time that the carbonate radical exists as an acid/base couple, $HCO_3^{\bullet}/CO_3^{\bullet -}$, with a p$K_a$ value ranging from *ca.* 7.9[7] to *ca.* 9.5.[8] However, the most recent studies rather indicate that the carbonate radical is a strong acid with p$K_a < 0$[9] or at least is negatively charged at neutral pH (meaning a pK_a value lower than 8).[10] In addition, the reactivity of carbonate radicals towards organic or inorganic compounds had been found to be pH-dependent[8] but this dependence has recently been demonstrated to be related to medium effects instead of dissociation of $HCO_3^{\bullet}$.[11]

Carbonate radicals present a significant and selective reactivity towards organic compounds. The first studies were published in the 70's by Hoffman *et al.*,[12–16] showing that carbonate radicals react with N-containing organic molecules (aniline derivatives, tryptophan...) with quite high second-order rate constants (10^7–10^9 M^{-1}.s^{-1}[12]). As electrophilic reagents, carbonate radicals efficiently react with electron-rich compounds. The reaction involves either an electron transfer or a hydrogen atom abstraction as proposed by Elango *et al.* for aliphatic amines and substituted anilines.[17,18] Recent studies have also been performed concerning the fate and evaluation of carbonate radical in field waters[19] or itsinfluence on water treatment processes using ozone.[20,21] It has been shown that its action could lead to efficient degradation of pesticides such as atrazine ($k = 4 \times 0^6$ M^{-1}.s^{-1}),[22]and fenthion or thioanisole ($k \approx 2 \times 10^7$ M^{-1}.s^{-1}).[23] In the case of thioanisole, the sulfone and sulfoxide derivatives have been identified and the mechanism of their formation is assumed to involve an electron transfer from a first $CO_3^{\bullet -}$, followed by O transfer with a second $CO_3^{\bullet -}$.[23,24] The carbonate radical may also react by hydrogen abstraction.[25]

Benzimidazole fungicides were introduced in the sixties and their use has considerably increased because of their high efficiency at low doses and their ability to inhibit the development of a wide variety of fungi. Carbendazim (methyl-2 benzimidazole carbamate, see its formula at the top of Scheme 1) is one of the most widely used systemic fungicides. As a result, it has been frequently detected in surface water.[26,27] Carbendazim hydrolysis is slow in the pH range of natural waters.[28] The phototransformation of carbendazim has been studied by different authors and they showed[29–32] that carbendazim is a quite stable molecule under UV irradiation. Transformation of organics by radicals ($HO^\bullet$ and/or $CO_3^{\bullet -}$) may be of significant importance in aquatic environments.

The study of carbonate reactivity is not easy to perform in a simple way. The H_2O_2/UV system provides a convenient

 DOI: 10.1039/b204332g

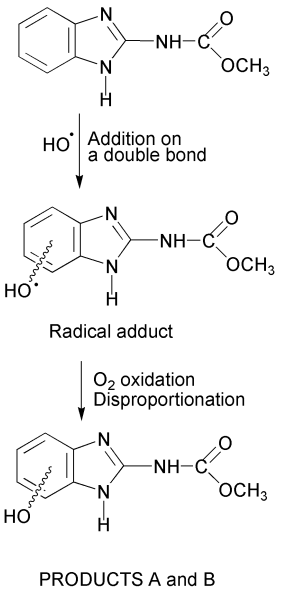

Scheme 1 First pathway for the reaction of HO• with carbendazim.

process to generate the hydroxyl radical, which further reacts with hydrogenocarbonate ion to generate the carbonate radical. Because of the existence of simultaneous reactions, kinetic modelling is a useful tool to evaluate the different reactivities.

In this work, the reactivity of hydroxyl and carbonate radicals towards carbendazim has been studied with particular attention to the kinetic aspects and the identification of by-products of the reactions.

Experimental

Carbendazim, sodium hydroxide, sodium perchlorate, perchloric acid, sodium hydrogenocarbonate and methanol were commercial products of the purest grade available. All solutions were prepared with purified water (Millipore Milli-Q). pH measurements were carried out with a Tacussel PHM 240. The ionic strength was not controlled unless otherwise mentioned.

The irradiation set-up was a batch photoreactor (volume of irradiated solution = 2 L, optical pathway = 3.6 cm). The lamp (Heraeus NN 40/20 low pressure mercury lamp) was located at the centre of the reactor, in a quartz sleeve. The photonic flux emitted by the lamp was evaluated with H_2O_2 as an actinometer as described elsewhere.[33] Actinometries were performed weekly. Typical values equal to $(6.0 \pm 0.5) \times 10^{-6}$ Einstein.L^{-1}.s^{-1} were obtained during the period of the experiments. Hydrogen peroxide concentration was measured by the Ti-complexometry method (Eisenberg[34]). Volumes of samples and reactants were adjusted for limiting volumes. UV-visible spectra and absorbance measurements were performed on a Safas double-beam spectrometer.

Carbendazim disappearance and formation of by-products was followed using high performance liquid chromatography (HPLC; Waters system equipped with a Waters 600 pump, a Waters 717 autosampler and a Waters 996 photodiode array detector). The column was purchased from Alltech (Kromasil C_{18} 250 mm–4.6 mm–5 μm) and the eluent was a mixture of methanol–water (50/50) or methanol–aqueous phosphate buffer (50/50 pH = 7.2). HPLC-mass spectrometry experiments have been performed at the "Service Central d'Analyses" of the CNRS (Lyon). The apparatus was a Hewlett–Packard HP1100-MSD system working in positive electrospray mode. The column was a Waters Xterra MSC18 (150 mm–2.1 mm) and the eluent was a mixture of methanol and H_3PO_4 acidified water.

All the experiments have been performed at least twice. The data shown are examples of the results.

Kinetic modelling was performed using Gepasi software.[35,36] The full set of chemical reactions used for the simulations is given in Table 1. C stands for carbendazim.

Results and discussion

H_2O_2/UV photolysis: background

Upon irradiation of hydrogen peroxide in aqueous solution at 254 nm, it is well-known that the homolytic scission of the O–O bond leads the formation of hydroxyl radicals according to reaction 1 in Table 1. The rate of hydrogen peroxide disappearance (hence the rate of HO• radical formation) according to reaction 1 is given by eqn. (I):

$$\frac{d[HO^\bullet]}{dt} = -2\frac{d[H_2O_2]}{dt} = 2\phi^{pri}_{H_2O_2} I_0 \frac{A_{H_2O_2}}{A_{tot.}}(1 - e^{-2.3\,A_{tot.}}) \quad (I)$$

where $\phi^{pri}{}_{H_2O_2}$ is the primary quantum yield of hydrogen peroxide photolysis (equal to 0.5[33]), I_0 is the photonic flux emitted by the lamp, determined by actinometry, $A_{H_2O_2} = \varepsilon[H_2O_2]l$ is the absorbance of H_2O_2 in solution (with ε—the molar absorption coefficient of H_2O_2—equal to 18.6 $M^{-1}.cm^{-1}$[33] and l the mean optical pathway for the photon) and $A_{tot.}$ is the absorbance of the solution at 254 nm: $A_{tot.} = l\{\varepsilon[H_2O_2] + \Sigma(\varepsilon_X[X])\}$; X stands for other absorbing species at 254 nm (including carbendazim).

Hydroxyl radicals disappear by four main reactions involving hydrogen peroxide (2), carbendazim (4), hydrogenocarbonate and carbonate ions (7 and 8 according to the presence of these species) and other scavengers present in our milli-Q water (5). So, the overall rate of HO• radical disappearance can be expressed by eqn. (II):

$$-\frac{d[HO^\bullet]}{dt} = (k_2[H_2O_2] + k_4[C] + k_7[HCO_3^-] + k_8[CO_3^{2-}] + k_5[S])[HO^\bullet] \quad (II)$$

Reactions (17) and (20) are neglected here (radical-radical reactions) and reaction 6 also because of its low rate constant and low abundance of H_2CO_3 in our experimental conditions. Similarly, the proportion of HO_2^- was less than 0.1% because our highest pH value was 8.6 (pK_a of H_2O_2/HO_2^- is 11.8). So its contribution (reaction 3) was neglected. However, these reactions and species are considered in the Gepasi calculations.

If we apply the steady-state hypothesis to hydroxyl radicals then relation (III) is obtained :

$$[HO^\bullet]_{ss} = \frac{2\phi^{pri}_{H_2O_2} \times I_0 \times \frac{A_{H_2O_2}}{A_{tot.}} \times (1 - e^{-2.3\,A_{tot.}})}{k_2[H_2O_2] + k_4[C] + k_7[HCO_3^-] + k_8[CO_3^{2-}] + k_5[S]} \quad (III)$$

In the presence of hydrogenocarbonate ions, one can suppose a reaction between carbonate radical (formed according to reactions 7 and 8) with carbendazim and the overall rate of carbendazim disappearance will be given by relation (IV) :

$$-\frac{d[C]}{dt} = \phi_C \frac{A_C}{A_{tot.}} I_0(1 - e^{-2.3\,A_{tot.}}) + k_4[C][HO^\bullet] + k_{12}[C][CO_3^{\bullet -}] \quad (IV)$$

where ϕ_C is the quantum yield of carbendazim disappearance (the molar absorption coefficients of carbendazim in aqueous solution are $\varepsilon_{254,NH^+} = 2330$ M^{-1} cm^{-1} and $\varepsilon_{254,N} = 4470$ M^{-1} cm^{-1} for the protonated and the neutral compound, respectively, and $pK_a = 4.53$[32]), A_C represents the fraction of light absorbed by carbendazim in the mixture and k_4 and k_{12}

Table 1 Chemical reactions involved in the system and used for the kinetic simulations

Reaction Number	Reaction	Rate or equilibrium constant	Reference
1	$H_2O_2 \xrightarrow{h\nu} 2\ HO^\bullet$	$\phi^{pri}_{H_2O_2} I_{a,H_2O_2}$	2
	Photochemical production of HO		
2	$HO^\bullet + H_2O_2 \rightarrow HO_2^\bullet + H_2O$	2.7×10^7 L.mol^{-1}.s^{-1}	37
3	$HO^\bullet + HO_2^- \rightarrow HO_2^\bullet + HO^-$	7.5×10^9 L.mol^{-1}.s^{-1}	37
4	$HO^\bullet + C \rightarrow$ Products	k_4	This work
	$HO^\bullet$ induced transformation		
5	$HO^\bullet + S^a \rightarrow$ Products	$k_5[S] \approx 2000 \pm 300$ s^{-1} (Milli-Q water)	This work
	Quenching of $HO^\bullet$ radicals		
6	$HO^\bullet + H_2CO_3^- \rightarrow CO_3^{\bullet-} + H_2O + H^+$	$< 10^6$ L.mol^{-1}.s^{-1}	40
7	$HO^\bullet + HCO_3^- \rightarrow CO_3^{\bullet-} + H_2O$	1.0×10^7 L.mol^{-1}.s^{-1}	40
8	$HO^\bullet + CO_3^{2-} \rightarrow CO_3^{\bullet-} + HO^-$	4.1×10^8 L.mol^{-1}.s^{-1}	40
9	$HO^\bullet + CH_3OH \rightarrow H_2O + {}^\bullet CH_2OH$	9.7×10^8 L.mol^{-1}.s^{-1}	1
10	$C(N) \xrightarrow{h\nu}$ Products	$\phi_C I_{a,C}$	32
	Direct phototransformation		
11	$CO_3^{\bullet-} + H_2O_2 \rightarrow HO_2^\bullet + HCO_3^-$	4.3×10^5–8×10^5 L.mol^{-1}.s^{-1}	41
12	$CO_3^{\bullet-} + C \rightarrow$ Products	k_{12}	This work
	$CO_3^{\bullet-}$ induced transformation		
13	$H_2O_2 + HO_2^\bullet \rightarrow HO^\bullet + H_2O + O_2$	2.5–5 L.mol^{-1}.s^{-1}	1
14	$HO_2^\bullet + HO_2^\bullet \rightarrow H_2O_2 + O_2$	8.3×10^5 L.mol^{-1}.s^{-1}	38
15	$HO_2^\bullet + O_2^{\bullet-} \rightarrow HO_2^- + O_2$	9.7×10^7 L.mol^{-1}.s^{-1}	38
16	$HO_2^\bullet \rightarrow O_2^{\bullet-} + H^+$	$k_{for} = 1.58 \times 10^5$ L.mol^{-1}.s^b	38
		$k_{back} = 10^{10}$ L.mol^{-1}.s^{-1}	
17	$HO^\bullet + HO^\bullet \rightarrow H_2O_2$	5.5×10^9 L.mol^{-1}.s^{-1}	1
18	$CO_3^{\bullet-} + CO_3^{\bullet-} \rightarrow O_2 + C_2O_4^{2-}$	1.4×10^7 L.mol^{-1}.s^{-1}	41
19	$CO_3^{\bullet-} + O_2^{\bullet-} \rightarrow CO_3^{2-} + O_2$	6.5×10^8 L.mol^{-1}.s^{-1}	41
20	$HO^\bullet + O_2^{\bullet-} \rightarrow HO^- + O_2$	7×10^9 L.mol^{-1}.s^{-1}	1
21	$H_2O \rightarrow H^+ + HO^-$	$k_{for} = 1.0 \times 10^{-4}$ L.mol^{-1}.s^{-1} ^{b}	39
		$k_{back} = 10^{10}$ L.mol^{-1}.s^{-1}	
22	$H_2O_2 \rightarrow H^+ + HO_2^-$	$k_{for} = 1.6 \times 10^{-2}$ L.mol^{-1}.s^{-1} ^{b}	3
		$k_{back} = 10^{10}$ L.mol^{-1}.s^{-1}	
23	$C(NH^+) \rightarrow C(N) + H^+$	$k_{for} = 2.95 \times 10^5$ L.mol^{-1}.s^{-1} ^{b}	32
		$k_{back} = 10^{10}$ L.mol^{-1}.s^{-1}	
24	$HCO_3^- \rightarrow CO_3^{2-} + H^+$	$k_{for} = 4.5 \times 10^{-1}$ L.mol^{-1}.s^{-1} ^{b}	39
		$k_{back} = 10^{10}$ L.mol^{-1}.s^{-1}	
25	$H_2CO_3^- \rightarrow HCO_3^- + H^+$	$k_{for} = 4.5 \times 10^3$ L.mol^{-1}.s^{-1} ^{b}	39
		$k_{back} = 10^{10}$ L.mol^{-1}.s^{-1}	

^{a} S corresponds to the scavengers that are not eliminated by the water purification system (COT < 0.1 mg.L^{-1}). ^{b} Because the Gepasi software[35,36] is dealing with both forward and back reactions, equilibria were split into two reactions. The rates k_{for} and k_{back} were chosen such that $K = k_{for}/k_{back}$, whereas one of the two was assumed to be high ($> 5 \times 10^9$ L.mol^{-1}.s^{-1}).

are the second-order rate constants of carbendazim reactions with hydroxyl and carbonate radicals, respectively.

Transformation of carbendazim by H_2O_2/UV in the absence of HCO_3^-

Kinetic study. When the concentration of hydrogen peroxide is high enough, all the photons are absorbed by H_2O_2 at 254 nm and the fraction of light absorbed by carbendazim in the mixture is negligible. The quantum yield of carbendazim direct phototransformation being low ($\phi_C < 0.3\%$[32]), the photolysis of carbendazim is negligible.

Under these experimental conditions and according to eqn. (I), the rate of hydrogen peroxide disappearance will be constant and given by relation (V) :

$$\frac{d[H_2O_2]}{dt} = \phi^{pri}_{H_2O_2} \times I_0 = -\frac{1}{2}\frac{d[HO^\bullet]}{dt} \qquad (V)$$

On the time scale of the experiments, the concentration of hydrogen peroxide can be considered constant and equal to its initial value (this has been experimentally verified). In the absence of hydrogenocarbonate ions, relation (III) becomes:

$$[HO^\bullet]_{ss} = \frac{2\phi^{pri}_{H_2O_2} \times I_0}{k_2[H_2O_2]_0} \qquad (VI)$$

because $k_2[H_2O_2]_0 \lll k_4[C] + k_7[HCO_3^-] + k_8[CO_3^{2-}] + k_5[S]$ in relation (III). The rate of carbendazim disappearance is:

$$-\frac{d[C]}{dt} = k_4[C][HO^\bullet]_{ss} = \frac{k_4 \times 2\phi^{pri}_{H_2O_2} \times I_0}{k_2[H_2O_2]_0}[C] \qquad (VII)$$

This latter equation shows that the disappearance of carbendazim upon irradiation of aqueous solutions containing a low concentration of carbendazim and a high concentration of hydrogen peroxide should be first-order with respect to carbendazim concentration.

Without UV irradiation, no change in carbendazim concentration is observed in the presence of hydrogen peroxide within our typical concentration range. Aqueous solutions of carbendazim ($[C]_0 \approx 1$ μM) and hydrogen peroxide ($[H_2O_2]_0 = 0.066$ M) have been irradiated at 254 nm at pH = 2.3 (adjusted with $HClO_4$) and at pH = 7.3 (adjusted with NaOH). These experiments were performed to check the reactivity of both forms of carbendazim (protonated and neutral), based on its pK_a value equal to 4.53.[32] No significant difference was observed concerning either carbendazim or hydrogen peroxide disappearance. This means that hydroxyl radicals react with quite similar rates with both forms of carbendazim.

Aqueous solutions of carbendazim ($[C]_0 \approx 1$ μM) and H_2O_2 (33–144 mM) have been irradiated at 254 nm at pH = 5.5. In agreement with eqn. (VII) and as it is demonstrated in Fig. 1,

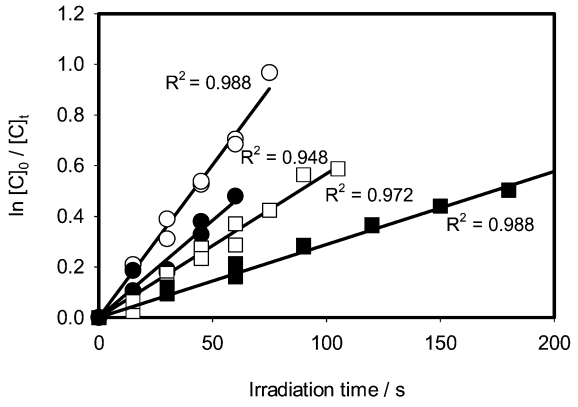

Fig. 1 Carbendazim disappearance upon irradiation at 254 nm of solutions containing high concentrations of H_2O_2: pH = 5.5, $[C]_0 \approx 1$ μM, $[H_2O_2]_0 = 33$ (○), 62 (●), 97 (□), 144 (■) mM. Solid lines correspond to linear regressions.

the disappearance of carbendazim obeys an apparent first-order kinetics law and the slope of the straight lines depends on $[H_2O_2]_0$. From these data, it is possible to calculate k_4 and a value equal to $(2.2 \pm 0.3) \times 10^9$ $M^{-1}.s^{-1}$ was obtained.

To check the accuracy of our kinetic modelling software, we have introduced the value determined for k_4 and we have run simulations for different hydrogen peroxide concentrations. Three examples of simulated curves are presented in Fig. 2. Note that it had been previously verified that the software was correctly simulating photochemical processes such as photolysis of carbendazim and hydrogen peroxide (these data are not shown in the paper). As previously mentioned, quenching of $HO^\bullet$ by scavengers present in our Milli-Q water (reaction 5) is negligible at high hydrogen peroxide concentration. We obtain a good agreement between experimental and simulated data for the four high hydrogen peroxide concentrations (33–144 mM: only one example is given in Fig. 2). When $[H_2O_2]_0$ is lower, the quenching of $HO^\bullet$ by species S cannot be neglected and we evaluate the product $k_5[S]$ by the use of the software. A mean value of $k_5[S]$ equal to 2000 ± 300 s^{-1} has been obtained for simulations run with different low hydrogen peroxide concentrations. After introduction in the software, we check that simulations give good results for low hydrogen peroxide starting concentrations (see the two examples given in Fig. 2 for 520 and 62 μM).

We did not take into account the formation and depletion of the carbendazim by-products in the kinetic model. Actually, we verified that if these products react with a second-order rate

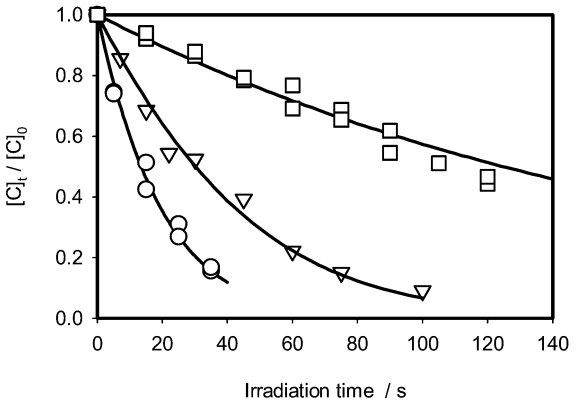

Fig. 2 Kinetics of carbendazim disappearance upon irradiation at 254 nm of aqueous solutions containing different concentrations of hydrogen peroxide. pH = 8.4 (adjusted with NaOH); $[C]_0 \approx 1$ μM; $[H_2O_2]_0 = 62$ (▽), 520 (○) μM, 97 (□) mM. Solid lines are simulated curves.

constant ranging between 5×10^8 and 5×10^9 $M^{-1}.s^{-1}$, there is no significant influence on the rate of carbendazim disappearance (the relative changes in carbendazim concentrations are lower than 2%).

The reactions of $HO_2^\bullet/O_2^{\bullet-}$ radicals and of $RO_2^\bullet$ radicals (eventually arising from reactions 2, 3 or 4, respectively) with carbendazim are not taken into account because they are thought to be negligible in our experimental conditions. This assumption seems to be confirmed by the good agreement obtained between the simulated and the experimental data in Fig. 2.

Identification of degradation products. An aqueous solution of carbendazim (10 μM) has been irradiated in the presence of hydrogen peroxide (0.5 M) at pH = 5.5. One hundred milliliters of the solution has been concentrated under reduced vacuum to 1 mL and analysed by HPLC. Several peaks appeared using UV and mass detection. It has been possible to propose a structure for most of the peaks (Table 2). The nature of the degradation products shows that there exists at least two sites of attack of the hydroxyl radical: the benzene part of the benzimidazole ring and protons of the methyl group. We also have to mention that we do not detect any formation of phenol, aniline, 1,2-diaminobenzene; these products were presumed to be potential degradation products.

None of the products listed in Table 2 is commercially available or easy to synthesise; it was not possible to precisely quantify their formation. It can only be seen that peaks corresponding to products A and B were of similar abundance as the peak of carbendazim itself, which seems to indicate that the process leading to their formation is the major one or eventually that these products are more stable than the other ones.

Mechanism of the $HO^\bullet$ radical transformation of carbendazim. Accordingly, the proposed degradation pathways are summarised in Schemes 1 and 2. Two reaction sites are possible.

Pathway I (Scheme 1). This process seems to be the major one because the chromatographic peaks corresponding to the two isomers clearly appeared to be the largest ones, either by UV or MS detection. This kind of reactivity is well-known. The electrophilic reagent $HO^\bullet$ reacts by addition to a double bond of the benzimidazole ring. The formation of the radical adduct followed by an oxidation or a disproportionnation[42] leads to the formation of hydroxylated carbendazim. It was not possible to determine the position of the hydroxyl group on the benzimidazole ring. Two chromatographic peaks were present, very close to each other, indicating the formation of the two more stable isomers.

Path II (Scheme 2). This pathway appears to be of minor importance. $HO^\bullet$ reacts by hydrogen abstraction from the methyl group to form an alkyl radical, which traps oxygen,

Table 2 Possible structure for the degradation products

Observed m/z	Formula	
207 (two major peaks)	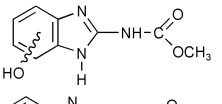	A, B (two isomers)
205 (traces)	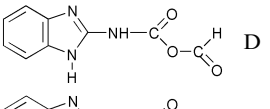	D
221 (traces)	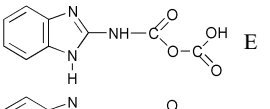	E
171 (traces)	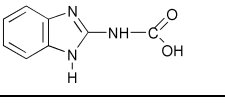	F

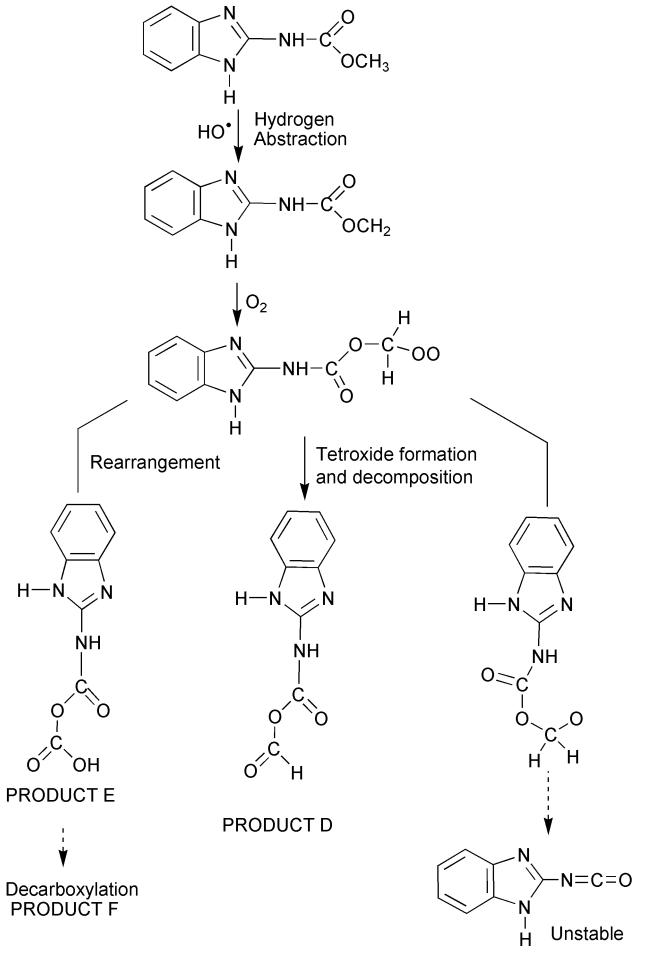

Scheme 2 Second pathway for the reaction of HO• with carbendazim.

leading to the formation of peroxyl radical. The evolution of the peroxyl radical *via* a bimolecular reaction leading to the formation of tetroxides was described by von Sonntag and Schuchmann.[43] At room temperature, tetroxides are unstable and undergo decomposition through different pathways.[43] It is possible to explain the formation of the observed degradation products. Peroxyl radicals are also able to trap a hydrogen atom, thus giving rise to hydroperoxide. The hydroperoxide compounds can evolve *via* classical β-fragmentations to product D as proposed by Fish.[44] Product F certainly arises from product E *via* decarboxylation. We were not able to detect the analogous product eventually formed by decarboxylation of product D.

Transformation of carbendazim by H_2O_2/UV in the presence of HCO_3^- : evidence for the involvement of carbonate radical

Hydrogen peroxide disappearance in the presence of HCO_3^-. Aqueous solutions containing hydrogen peroxide ($[H_2O_2]_0 \approx$ 500 μM) and different concentrations of hydrogenocarbonate ions (0–20 mM) have been irradiated at 254 nm. The pH of the solution was 8.4 ± 0.2 in the presence of HCO_3^- or when adjusted with NaOH. The experimental data are shown in Fig. 3. (It was verified that hydrogenocarbonate ions do not absorb light at 254 nm).

As evidenced, there is no significant effect of the addition of hydrogenocarbonate ions : the experimental hydrogen peroxide concentrations are almost the same within experimental error for the same irradiation time, whatever the hydrogenocarbonate ions concentration (the individual symbols are overlapped). In Fig. 3, we plot two simulations of the disappearance of hydrogen peroxide obtained with the

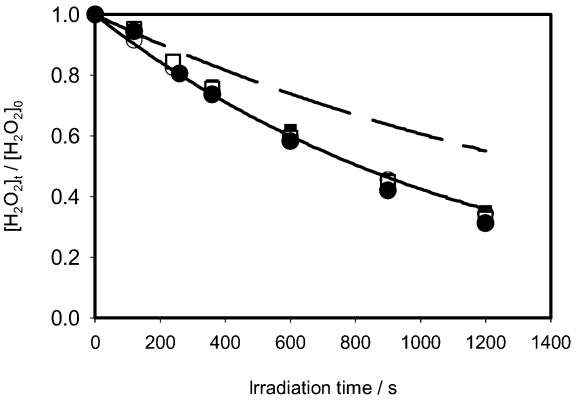

Fig. 3 Kinetics of H_2O_2 disappearance upon irradiation of aqueous solutions containing hydrogenocarbonate ions. $[HCO_3^-]_0 = 0$ (○), 5 (■), 10 (□), 20 (●) mM. Lines are simulated curves (see text).

second-order rate constant k_{11} for the reaction between carbonate radical and H_2O_2 set to 0 M^{-1} s^{-1}(dashed line) or to 6.1×10^5 $M^{-1}.s^{-1}$ (full line). This latter value corresponds to the mean of the reported values.[41] The second value fits very well with the experimental data, indicating that the contribution of carbonate radical to the disappearance of H_2O_2 is of significant importance. Actually, the disappearance of hydrogen peroxide due to reaction 11 completely compensates the quenching of HO• radicals with H_2O_2 (reaction 2) in the presence of HCO_3^- (reactions 7 and 8). Additionally, the absence of variation with hydrogenocarbonate concentration indicates that a higher quenching of reaction 2 exactly corresponds to a higher occurrence of reaction 11.

It is worth noting that no significant change is observed between simulations performed with $k_{11} = 4.3 \times 10^5$ $M^{-1}.s^{-1}$ or or $k_{11} = 8.0 \times 10^5$ $M^{-1}.s^{-1}$, the two values that are generally used in the literature. It should be noted that more recently, Nemes *et al.* proposed a value 10^3 times higher for this reaction [$k_{11} = (7.6 \pm 0.7) \times 10^8$ = L.mol^{-1} s^{-1}].[20] This may be due to the high pH at which the experiments were performed (pH > 10.7), thus implying significant reaction with the anion HO_2^-.

Carbendazim disappearance in the presence of HCO_3^-. As previously mentioned, the reactions of hydrogenocarbonate and carbonate ions with HO• leads to a decrease of the rate of carbendazim degradation. The experiments have been performed with five concentrations in HCO_3^-. Even if our initial preoccupation was related to environmental aquatic waters, we extended our experiments to a wider range of hydrogenocarbonate ion concentrations than those typically met. In Fig. 4 is represented the percentage of carbendazim transformed during a 50 s

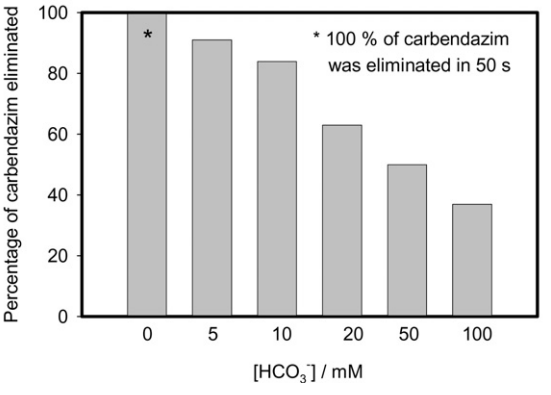

Fig. 4 Percentage of carbendazim eliminated upon irradiation at 254 nm of aqueous solutions for 50 s: $[C]_0 \approx 1$ μM, $[H_2O_2]_0 \approx 500$ μM, pH = 8.4 ± 0.2.

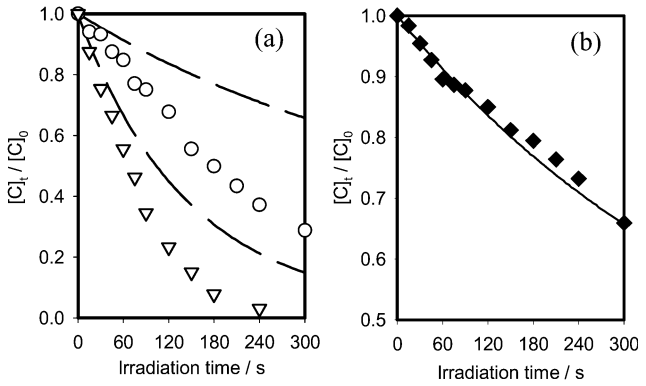

Fig. 5 Kinetics of carbendazim disappearance upon irradiation: $[H_2O_2]_0 \approx 500$ μM, $[C]_0 \approx 1$ μM, pH = 8.4 ± 0.2. (a) $[HCO_3^-]_0 = 5$ (□), 10 (▽), 20 (■), 50 (○), 100 (●) mM; dashed lines are simulations with $k_{12} = 0$ $M^{-1}.s^{-1}$. (b) $[CH_3OH]_0 = 0.65$ (◆) mM; solid line is a simulation.

irradiation of an aqueous solution containing hydrogen peroxide and different concentrations of hydrogenocarbonate ions.

The results show that the higher the concentration of HCO_3^-, the lower the extent of carbendazim degradation. This expected result is in good agreement with the quenching effect of hydrogenocarbonate ions. Hydroxyl radicals competitively react with hydrogenocarbonate and carbonate ions instead of carbendazim. Simulations for this set of experiments were performed.

The first simulations for two concentrations of hydrogenocarbonate ions ($[HCO_3^-]_0 = 10$ mM or 50 mM) are shown as dashed lines in Fig. 5(a). As evidenced, these simulations lead to an underestimation of the rate of carbendazim disappearance. To check that the software was correctly taking into account the scavenging effect, experiments have been run using methanol instead of hydrogenocarbonate as an $HO^\bullet$ trap ($k_9 = 9.7 \times 10^8$ $M^{-1}.s^{-1}$). The concentration of methanol was chosen to have $k_9[MeOH] = k_7[HCO_3^-] + k_8[CO_3^{2-}] = 6.3 \times 10^5$ s^{-1}, that is to have the same "quenching strength" as the solution containing 50 mM of hydrogenocarbonate ions. The results are presented in Fig. 5(b) and it is evident that the model predicts very well the degradation of carbendazim in the presence of methanol. This indicates that the quenching effect was correctly simulated in the presence of methanol but not in the presence of hydrogenocarbonate. According to this set of results, the existence of a supplementary route for carbendazim degradation in the system $H_2O_2/UV/HCO_3^-$ can be put forward.

Taking into account the experimental conditions, the additional reaction should involve the carbonate radical. We performed successive simulations to evaluate the second-order rate constant between carbonate radical and carbendazim using iterations to reach a minimum gap between the experimental and the calculated data. The best fits were obtained using $k_{12} = (6 \pm 2) \times 10^6$ $M^{-1}.s^{-1}$ (mean of 15 experiments performed with the five different concentrations of HCO_3^-). This value is significantly lower than the one corresponding to the second-order rate constant between $HO^\bullet$ and carbendazim but it is well-known that carbonate radical is less reactive and more selective than the hydroxyl radical. Using the above-mentioned value for k_{12}, simulations (solid lines, Fig. 6) correctly fit the experimental data.

In the presence of hydrogenocarbonate ions, carbendazim disappears by three different processes: photolysis, $HO^\bullet$ radicals induced transformation and a process involving carbonate radicals. By using the simulations and assuming that each process leads to the formation of a unique and specific degradation product, the respective contributions of each process were estimated. The results are summarised in Fig. 7. Photochemical direct transformation is negligible in the presence of the other two processes. This is due to the low rate of light absorption by carbendazim and also to the low efficiency of the phototransformation (quantum yield $\phi_C < 0.3\%$[32]).

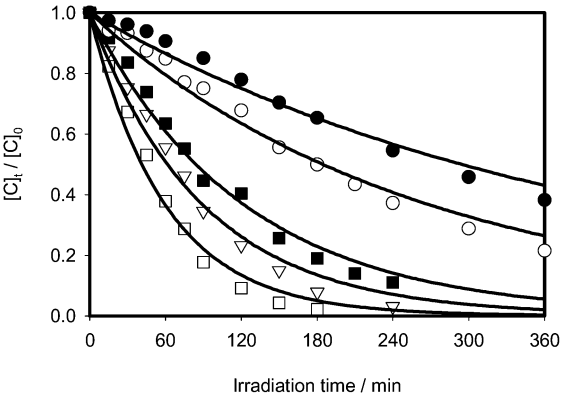

Fig. 6 Kinetics of carbendazim disappearance upon irradiation at 254 nm of aqueous solutions containing: $[H_2O_2]_0 \approx 500$ μM, $[C]_0 \approx 1$ μM, pH = 8.4; $[HCO_3^-]_0 = 5$ (□), 10 (▽), 20 (■), 50 (○), 100 (●) mM; solid lines are simulations with $k_{12} = (6 \pm 2) \times 10^6$ $M^{-1}.s^{-1}$.

As evidenced in Fig. 7, the involvement of $HO^\bullet$ in carbendazim degradation decreases as the concentration of HCO_3^- increases. This is in agreement with the strong quenching effect of hydrogenocarbonate/carbonate ions. The transformation induced by carbonate radical represents the major route of carbendazim disappearance. At low hydrogenocarbonate ion concentrations (< 10 mM), the percentage of carbendazim degradation due to the carbonate radicals is *ca.* 30–40% which is of significant importance with regard to natural waters.

Degradation products of carbendazim in the presence of HCO_3^-. HPLC-MS experiments show that only degradation products A and B (see Table 2) are formed. However, we were not able to determine if the formation of these products is due

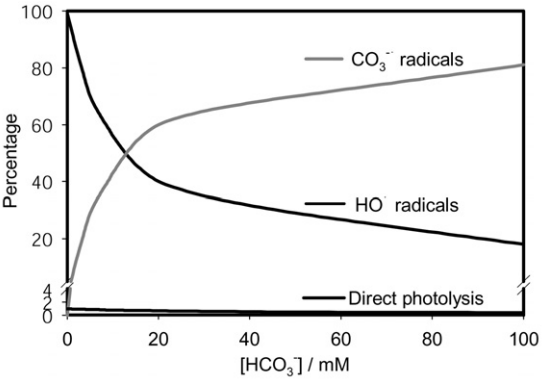

Fig. 7 Evaluation of the different degradation pathways of carbendazim as a function of $[HCO_3^-]_0$.$[H_2O_2]_0 \approx 500$ μM, pH = 8.4 ± 0.2, $[C]_0 \approx 1$ μM. Irradiation at 254 nm.

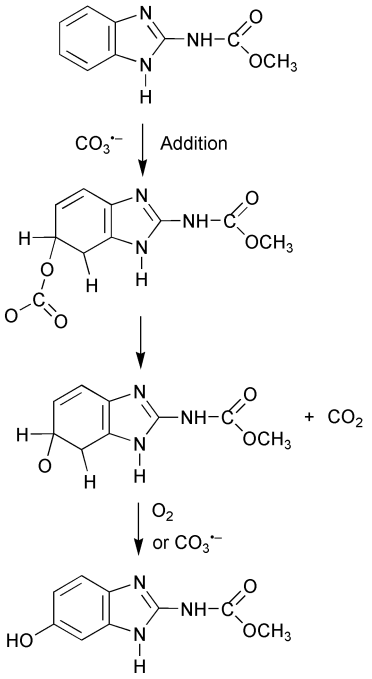

Scheme 3 Possible pathway for the reaction of $CO_3^{\bullet -}$ with carbendazim leading to the formation of one of the products A or B.

to reaction with carbonate radicals or with hydroxyl radicals. A possible reaction pathway involving reaction of $CO_3^{\bullet -}$ with carbendazim can be proposed as indicated in Scheme 3. In addition, we cannot exclude reaction of carbonate radicals by electron transfer with the nitrogen atom but this reaction would more likely lead to the breakdown of the imidazole ring and the formation of lower molecular weight intermediates.

Conclusion

The transformation of the fungicide carbendazim by hydroxyl radicals (generated by the H_2O_2/UV system) has been studied. In the presence of high concentrations of hydrogen peroxide, the second-order rate constant of the reaction of $HO^{\bullet}$ radicals with carbendazim has been determined to be equal to $(2.2 \pm 0.3) \times 10^9$ L.mol^{-1}.s^{-1}. Hence, this value has been introduced into a kinetic model and the disappearance of carbendazim can be well simulated over a wide range of hydrogen peroxide concentrations (50 μM–150 mM). The main site of hydroxyl radical reaction is the benzene ring of the benzimidazole part of carbendazim, leading to the formation of hydroxylated derivatives. Degradation products corresponding to reaction of the hydroxyl radical with the methyl carbamate group have been identified but this path represents only a minor route of carbendazim disappearance. In the presence of hydrogenocarbonate ions, kinetic modelling gives evidence for the involvement of additional pathways for carbendazim degradation besides direct photolysis and $HO^{\bullet}$ radical induced transformation. According to our results, it implies the carbonate radical. Our kinetic model led to an estimated value equal to $(6 \pm 2) \times 10^6$ M^{-1}.s^{-1} in the concentration and pH ranges of our study. This reactivity must not be neglected with regards to environmental or water treatment processes.

References

1 G. V. Buxton, C. L. Greenstock, W. P. Helman and A. B. Ross, *J. Phys. Chem. Ref. Data*, 1988, **17**, 516–818.
2 S. Lunak and P. Sedlak, *J. Photochem. Photobiol. A: Chem.*, 1992, **68**, 1–33.
3 J. De Laat, P. Berger, T. Poinot, N. Karpel vel Leitner and M. Doré, *Ozone Sci. Eng.*, 1997, **19**, 395–408.
4 M. Hugül, R. Apak and S. Demirci, *J. Hazard. Mat.*, 2000, **77**, 193–208.
5 S. R. Cater, M. I. Stefan, J. R. Bolton and A. Safarzadeh-Amiri, *Environ. Sci. Technol.*, 2000, **34**, 659–662.
6 R. E. Huie, L. C. T. Shoute and P. Neta, *Int. J. Chem. Kinet.*, 1991, **23**, 541–552.
7 T. E. Eriksen, J. Lind and G. Merenyi, *Radiat. Phys. Chem.*, 1985, **26**, 197–199.
8 Z. Zuo, Z. Cai, Y. Katsumura, N. Chitose and Y. Muroya, *Radiat. Phys. Chem.*, 1999, **55**, 15–23.
9 G. Czapski, S. V. Lymar and H. A. Schwarz, *J. Phys. Chem. A*, 1999, **103**, 3447–3450.
10 R. H. Bisby, S. A. Johnson, A. W. Parker and S. M. Tavender, *J. Chem. Soc., Faraday Trans.*, 1998, **94**, 2069–2072.
11 S. V. Lymar, H. A. Scharz and G. Czapski, *Radiat. Phys. Chem.*, 2000, **59**, 387–392.
12 S. N. Chen, V. W. Cope and M. Z. Hoffman, *J. Phys. Chem.*, 1973, **77**, 1111–1116.
13 S. N. Chen, M. Z. Hoffman and G. H. Parson, Jr., *J. Phys. Chem.*, 1975, **79**, 1911–1912.
14 S. N. Chen and M. Z. Hoffman, *Radiat. Res.*, 1975, **62**, 18–27.
15 S. N. Chen and M. Z. Hoffman, *Radiat. Res.*, 1973, **56**, 40–47.
16 S. N. Chen and M. Z. Hoffman, *J. Phys. Chem.*, 1974, **78**, 2099–2102.
17 T. P. Elango, V. Ramakrishnan, S. Vancheesan and J. C. Kuriacose, *Proc. Indian Acad. Sci. (Chem. Sci.)*, 1984, **93**, 47–52.
18 T. P. Elango, V. Ramakrishnan, S. Vancheesan and J. C. Kuriacose, *Tetrahedron*, 1985, **41**, 3837–3843.
19 J. Huang and S. A. Mabury, *Environ. Toxicol. Chem.*, 2000, **19**, 2181–2189.
20 A. Nemes, I. Fabian and R. van Eldik, *J. Phys. Chem. A*, 2000, **104**, 7995–8000.
21 J. L. Acero and U. von Gunten, *Ozone Sci. Eng.*, 2000, **22**, 305–328.
22 J. Huang and S. A. Mabury, *Environ. Toxicol. Chem.*, 2000, **19**, 1501–1507.
23 J. Huang and S. A. Mabury, *Chemosphere*, 2000, **41**, 1775–1782.
24 J. Lilie, R. J. Hanrahan and A. Hengkein, *Radiat. Phys. Chem.*, 1978, **11**, 225–227.
25 C. L. Clifton and R. E. Huie, *Int. J. Chem. Kinet.*, 1993, **25**, 199–203.
26 A. Oubina, E. Martinez, J. Gascon, D. Barcelo and I. B. De Alleluia, *Int. J. Environ. Anal. Chem.*, 1998, **70**, 75–91.
27 M. Loewy, V. Kirs, G. Carvajal, A. Venturino and A. M. Pechen De d'Angelo, *Sci. Total Environ.*, 1999, **255**, 211–218.
28 C. Tomlin, *The Pesticide Manual*, British Crop Protection Council, Bracknell, London, 10th edn., 1994.
29 W. M. Abdou, M. R. Mahran, M. M. Sidky and H. Wamhoff, *Chemosphere*, 1985, **14**, 1343–1353.
30 W. M. Abdou, M. R. Mahran, M. M. Sidky and H. Wamhoff, *Chemosphere*, 1986, **15**, 1063–1071.
31 R. Panades, A. Ibarz and S. Esplugas, *Water Res.*, 2000, **34**, 2951–2954.
32 P. Mazellier, E. Leroy and B. Legube, *J. Photochem. Photobiol. A: Chem.*, 2002, **153**, 221–227.
33 I. Nicole, J. De Laat, M. Doré, J. P. Duguet and C. Bonnel, *Water Res.*, 1990, **24**, 157–168.
34 G. M. Eisenberg, *Ind. Eng. Chem. Anal.*, 1943, **15**, 327–328.
35 P. Mendes, *Comp. Appl. Biosci.*, 1993, **9**, 563–571.
36 P. Mendes, *Trends Biochem. Sci.*, 1997, **22**, 361–363.
37 H. Christensen, K. Sehested and H. Corfitzen, *J. Phys. Chem.*, 1982, **86**, 1588–1590.
38 B. H. Bielsi, D. E. Cabelli, R. L. Caruda and A. B. Ross, *J. Phys. Chem. Ref. Data*, 1985, **14**, 1041–1077.
39 W. Stumm and J. J. Morgan, *Aquatic Chemistry*, Wiley Interscience, New York, 3rd edn., 1996 (ISBN 0-471-51184-6).
40 G. V. Buxton, N. D. Wood and S. Dyster, *J. Chem. Soc., Faraday Trans. 1*, 1988, **84**, 1113–1121.
41 P. Neta, R. E. Huie and A. B. Ross, *J. Phys. Chem. Ref. Data*, 1988, **17**, 1065–1079.
42 U. Stafford, K. A. Gray and P. V. Kamat, *J. Phys. Chem.*, 1994, **98**, 6343–6350.
43 C. von Sonntag and H.-P. Schuchmann, *Angew. Chem., Int. Ed. Engl.*, 1991, **30**, 1229–1253.
44 A. Fish, in *Organic Peroxides*, ed. D. Svern, Wiley Interscience, John Wiley & Sons, New York, 1970, pp. 141–200.